JOURNAL OF MATERIALS SCIENCE 27 (1992) 1683–1689

Indentation behaviour of alloyed zirconia ceramics

J. T. CZERNUSZKA*, T. F. PAGE‡
Department of Metallurgy and Materials Science, University of Cambridge, Pembroke Street, Cambridge CB2 3QZ, UK

The hardness behaviour of four partially stabilized zirconias has been examined as a function of load and temperature. For all materials, it was found that as the load was decreased the hardness increased, by up to 50%. However, a further reduction in load caused a drastic reduction in hardness. The degree of this near-surface softening could be correlated to the proportion of tetragonal phase present. As the temperature of indentation was increased the hardness decreased. Irrespective of alloying and ageing, the hardness values tended towards the same value at the eutectoid temperature.

1. Introduction

Some alloyed zirconia ceramics are successfully replacing other ceramic components in wear-resistant applications. There are several reasons for this choice, which include: high toughness, thermal shock resistance, chemical stability and low coefficients of friction. As yet, however, little research has been reported on another important wear parameter, namely hardness, especially over the temperature range at which extrusion dies, engines, etc., operate. This paper seeks to redress the balance and shows how the hardness of two alloyed zirconias is dependent on load, temperature and microstructure.

2. Experimental procedure

2.1. Materials

Two zirconia samples were obtained, one containing ~ 2 wt % MgO (MPSZ), the other ~ 4 wt % CaO (CPSZ) as stabilizing agents. MPSZ was in the sub-eutectoid aged condition and is similar to that described by Hannink and Garvie [1]. CPSZ was received in the as-fired state (CPSZ0), consequently sections were aged in air at 1300 °C for 64 h (CPSZ64) and 100 h (CPSZ100). The evolution of the microstructure for these latter materials has been described by Hannink *et al.* [2], and for this particular composition should result in peak-aged and over-aged materials. Microstructural and phase data are presented in Table I.

Specimens were polished flat on a succession of diamond-impregnated laps and cloths. Cathodoluminescence (CL) mode imaging in the SEM was particularly useful in determining the distributions of the monoclinic phase. As an example, an edge of CPSZ64 is shown in Fig. 1. The light regions are the monoclinic phase. This material is supposed to contain only minimal amounts of this phase and its presence may be the result of evaporation of the stabilizer [3]. Such regions were avoided in these experiments.

2.2. Indentation testing

Two types of indentation tests under ambient conditions were performed. The first employed a Vickers indentor to examine any indentation size effect (ISE) [4]; the second used a Knoop indentor with which the near-surface hardness values could be ascertained. The Knoop indentor has a length: depth ratio of 30:1 compared with 7:1 for that of the Vickers indentor,

TABLE I Microstructural data of the zirconia samples

Material	Ageing conditions	Grain size (μm)	Phase distributions (%)		
			cubic	tetragonal	monoclinic
MPSZ	Sub-eutectoid	36	22	54	25
CPSZ0	As-fired	40	32	59	8
CPSZ64	1300°C for 64 h	40	38	43	18
CPSZ100	1300°C for 100 h	40	46	10	44

* *Present address*: Department of Materials, University of Oxford, Parks Road, Oxford OX1 3PH, UK.
‡ *Present address*: Department of Metallurgy and Engineering Materials, The University, Newcastle-upon-Tyne NE1 7RU, UK.

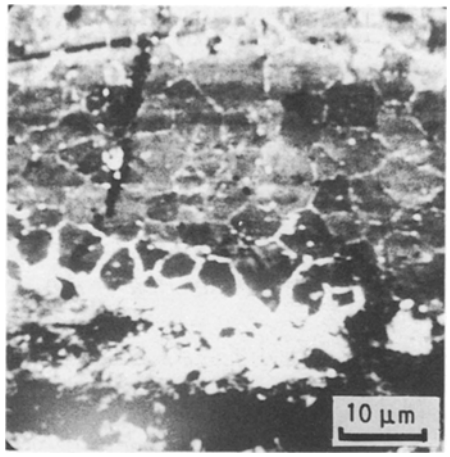

Figure 1 CL SEM mode image of the edge of CPSZ64. The bright regions are monoclinic phase.

such that for a similar diagonal the penetration is much reduced.

Further experiments were performed in an evacuated high-temperature hardness machine fitted with a Vickers indentor at a load of 1 kg. Temperatures up to 800 °C were used. Details of the operation of this machine are given in Naylor and Page [5].

3. Results

3.1. Room-temperature hardness behaviour

The variation of Vickers hardness with indentation diagonal is presented in Fig. 2. There are three reasons for plotting the data in this way (rather than as a function of load). Firstly, the indentation size effect index is more easily appreciated; secondly, the effect of microstructure on the measured hardness values may be evaluated; thirdly, the "effective" hardness at a given comparable wear track width may be easily compared.

In all cases, hardness increases with decreasing contact size (i.e. load). The values for CPSZ64 and CPSZ100 tend to converge, whereas that of MPSZ diverges from CPSZ64 at the lowest loads. Such behaviour is most easily denoted by the ISE index which is tabulated in Table II along with hardness values calculated at a constant indentation diagonal of 10 μm, $H_{10\mu m}$. The only exception to this behaviour is that for CPSZ0 which for the lowest loads decreases markedly. The value of the ISE index for this material excludes these near surface values.

The near surface hardness effects were examined further and the results plotted in Fig. 3. A similar increase in hardness with decreasing load (in this case plotted as a penetration depth) to Fig. 2 is observed until at a critical, materially dependent depth, a decrease is observed. Again, this is most marked for CPSZ0, which possesses the highest hardness value over most of the load range, but a similar value to that of CPSZ100 at 5 g. These low load values are also given in Table II.

3.2. Temperature variation of hardness

The results of the hardness versus temperature experiments are plotted in Fig. 4. For MPSZ, it can be seen that the hardness falls rapidly with temperature

TABLE II Hardness characterization (± 1 S.D.)

	Hardness			
	Vickers (kgf mm^{-2})		Knoop (kgf mm^{-2})	
Material	1 kg load	10 μm	10 g	ISE index
MPSZ	1178 ± 24	1626 ± 85	1192 ± 102	1.78 ± 0.1
CPSZ0	1400	2143	1121	1.67
CPSZ64	1250	1523	1683	1.78
CPSZ100	912	1483	1150	1.71

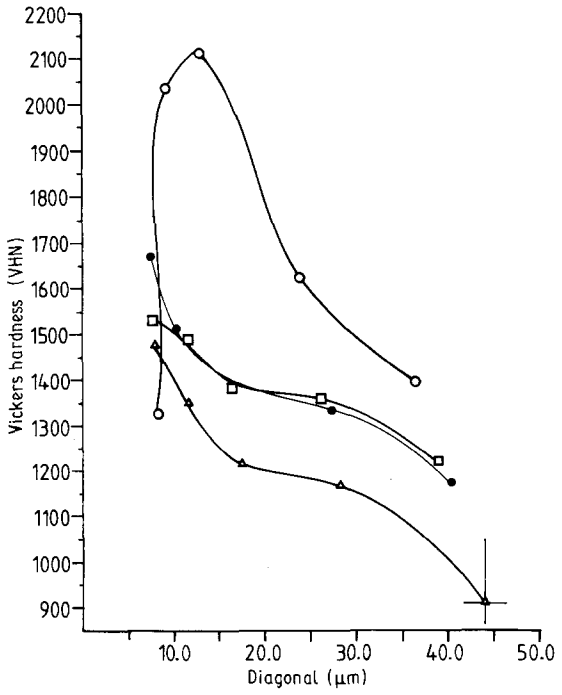

Figure 2 Plot of room-temperature Vickers hardness versus indentation diagonal. (○) CPSZ0; (□) CPSZ64; (△) CPSZ100; (●) MPSZ.

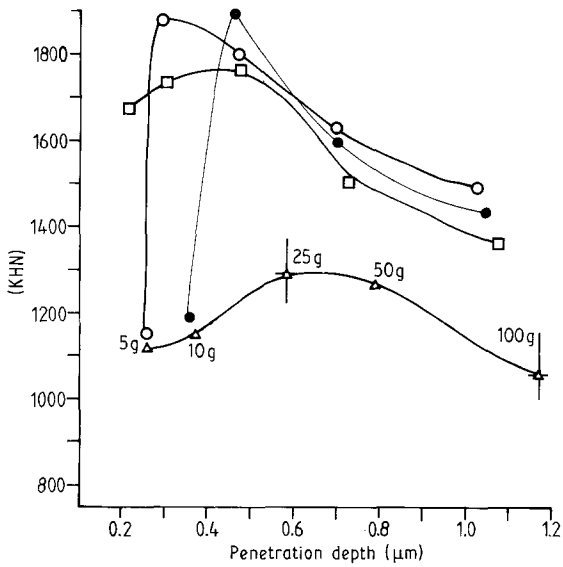

Figure 3 Plot of room-temperature Knoop hardness versus penetration depth. (○) CPSZ0; (□) CPSZ64; (△) CPSZ100; (●) MPSZ.

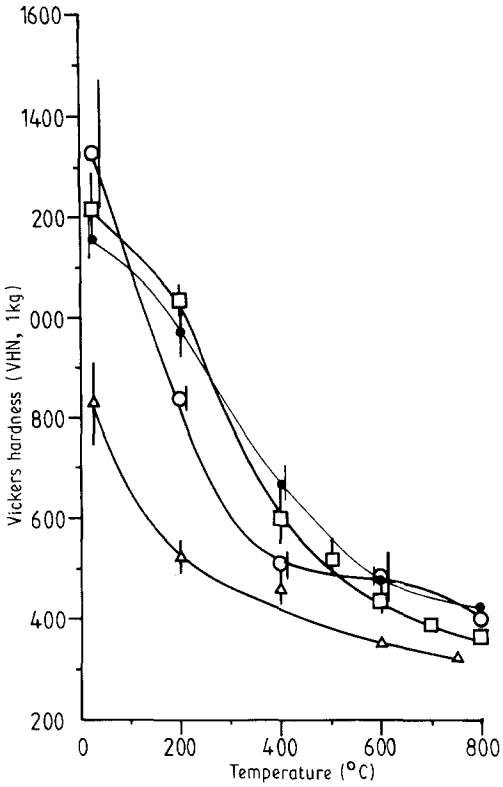

Figure 4 Plot of Vickers hardness at a load of 1 kg versus temperature. (○) CPSZ0; (□) CPSZ64; (△) CPSZ100; (●) MPSZ.

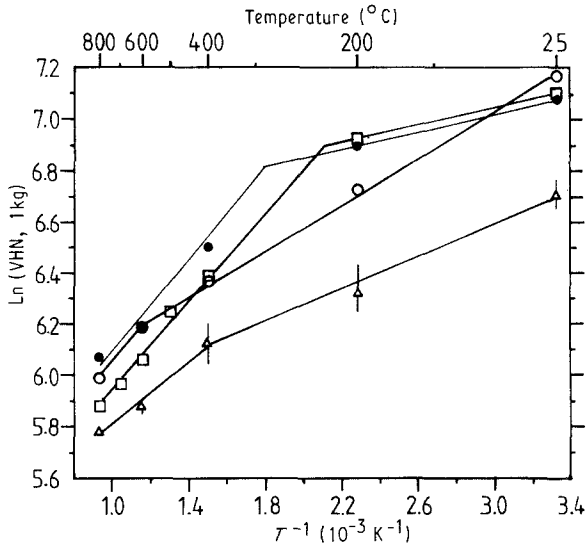

Figure 5 Arrhenius plot of hardness versus temperature behaviour. (○) CPSZ0; (□) CPSZ64; (△) CPSZ100; (●) MPSZ.

TABLE III Activation energies and critical temperatures (determined from Fig. 5)

Material	Critical temperature (°C)	Activation energy (kJ mol^{-1})	
		Low temperature	High temperature
MPSZ	557	13.2	71.3
CPSZ0	873	37.3	74.2
CPSZ64	476	13.5	52.6
CPSZ100	673	26.6	68.8

from room temperature to ~ 600 °C and then begins to level off. CPSZ0 and CPSZ100 possess similar behaviour to MPSZ in that there is an initial large decrease in hardness with increasing temperature, followed by a gradual levelling off; in this case, though, this occurs at ~ 400 °C. CPSZ64 possesses slightly different behaviour. A marked decrease in temperature is only observed above 200 °C with a more gradual levelling off at the higher temperatures. Between 200 and 400 °C it possesses the highest hardness of the three CPSZ materials.

It is possible to extract further information from the hardness: temperature data by assuming an Arrhenius-type behaviour

$$H = H' \exp(-Q/RTm)$$

where H' is a constant, Q is an activation energy and m is a creep exponent and is generally found to be about 10 [6]. Fig. 5 plots the results represented to fit this equation. There are two regimes of hardness temperature separated by a critical temperature. Activation energies calculated from the slopes of such curves are given in Table III, together with the corresponding critical temperatures.

3.3. Microscopical examination

To determine the mode of deformation over the temperature range, a microscopical examination of the indentation-associated deformation was performed. The principal technique was scanning electron microscopy (SEM) in the secondary electron (SE), backscattered (BS) and CL modes.

Fig. 6 shows an indentation in MPSZ made at room temperature. It has been ion-beam etched (5 keV, argon ions). Fig. 6a and b are complementary BS and CL images. The four lobes surrounding the indentation in Fig. 6b are monoclinic material and have been previously described [7]. Fig. 7 shows an indentation in the same material made at 800 °C. Fig. 7a and b are, respectively, SE and CL images of the same region. It is now noticeable that the indentation-induced monoclinic transformation is restricted to the centre of the indentation; no lobes were observed.

Turning to the CPSZ materials, other striking features were observed. Fig. 8 shows the interaction of the fracture paths with the grain boundaries. Also evident are faint shear bands (e.g. [8]), and regions of suppressed CL response. Fig. 9 examines how these shear bands are affected by grain boundaries. Fig. 9a is of a 10 g indentation within a grain centre exhibiting well-defined shear bands. Fig. 9b is of an indentation within a corner of a grain and almost complete band suppression is obtained. Fig. 9c is of an indentation on a grain boundary; bands are now observed within only the left-hand grain. Polishing damage (Fig. 9d) seems to suppress band formation. As the temperature is increased, the suppression of the CL signal from within the indentation itself is reduced, Fig. 10, and it is now merely outlined. No shear bands were observed in CPSZ64 and CPSZ100.

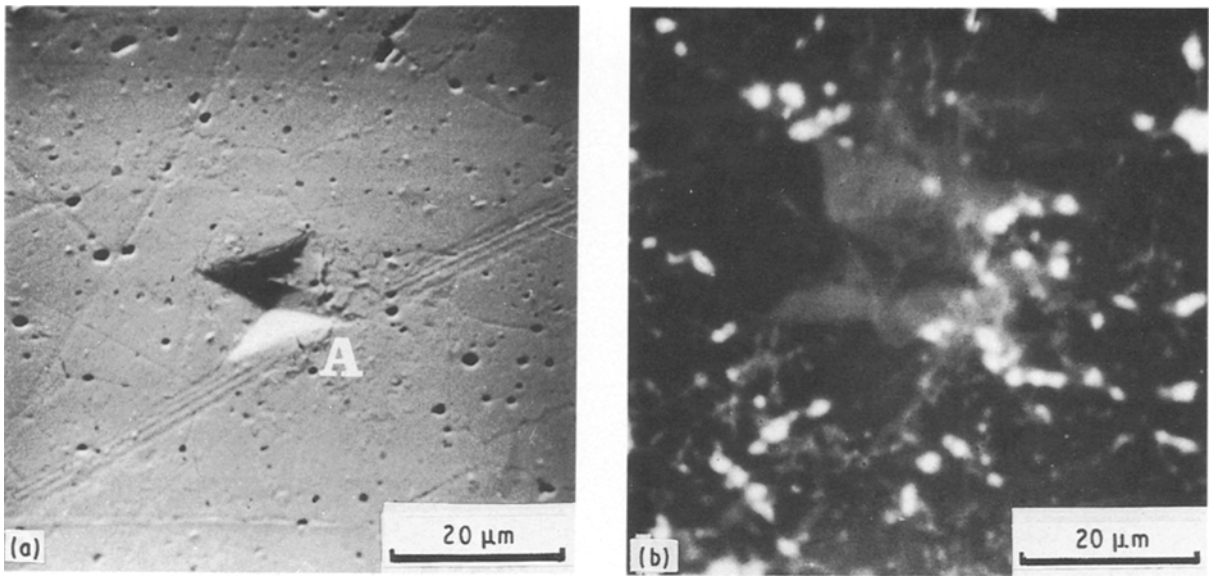

Figure 6 (a) SE and (b) CL SEM images of a 1 kg Vickers indentation made at room temperature in MPSZ.

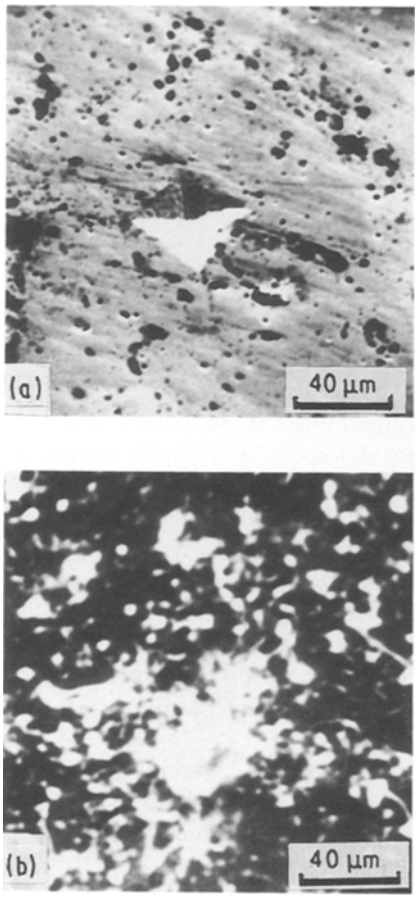

Figure 7 (a) SE and (b) CL SEM images of a 1 kg Vickers indentation made at 800 °C in MPSZ.

4. Discussion

The results and observations described above will now be discussed. The hardness:contact size dependencies presented in Fig. 2 show that the ranking of hardness values can alter depending on the scale of the contact. Thus, if a material was being chosen for a wear-resistant application purely on its hardness value, then it would be desirable to know the scale of the contact to be expected before proposing a material for a given purpose. In fact, most contacting situations are on a smaller scale than shown in Fig. 2, so Fig. 3 might be more appropriate. In this instance, for very shallow contacts CPSZ64 would be expected to have the highest wear resistance for plasticity dominated wear. This is indeed found to be the case and the results will be published at a later date.

The hardness at a load of 1 kg (i.e. a "macro-hardness") may be compared with the phase compositions of Table I. CPSZ0, with the highest cubic phase, has the highest hardness and CPSZ100, with the highest monoclinic phase, the lowest hardness. This is in agreement with Stevens [9] and Ingel *et al.* [10] where the hardness of the cubic phase is found to be slightly harder than that of the tetragonal phase, which in turn is much harder than the monoclinic. For the shallowest penetrations of Fig. 3, of course, no such correlation exists. However, in this case it is apparent that the materials with the greatest proportion of tetragonal phase suffer the least surface softening. It is known from infrared spectroscopic studies [11] that water is present on these surfaces and it could well be that this is a contributory factor to the surface softening (i.e. an environmentally sensitive hardness response [12]). Hence, on comparing Fig. 3 and Table I it seems that the tetragonal phase has the least enviromentally sensitive behaviour.

The hardness versus temperature data also show that the ranking of hardness values may be changed by an appropriate choice of temperature (see Fig. 4). At the highest temperatures, though, the three CPSZ samples tend to a similar value of ~ 270 VHN at $\sim 1200\,^{\circ}C$, which is the tetragonal eutectoid temperature. For MPSZ this is higher at $\sim 1400\,^{\circ}C$ and a corresponding extrapolated value of ~ 320 VHN. This latter value similar to that observed by Hannink and Swain [13]. The activation energies (see Table III) are, in general, lower than those of Hannink and Swain [13], who obtained values between 5 and 48 kJ mol^{-1}, depending on the temperature. This discrepancy is, in part, due to their use of an unheated

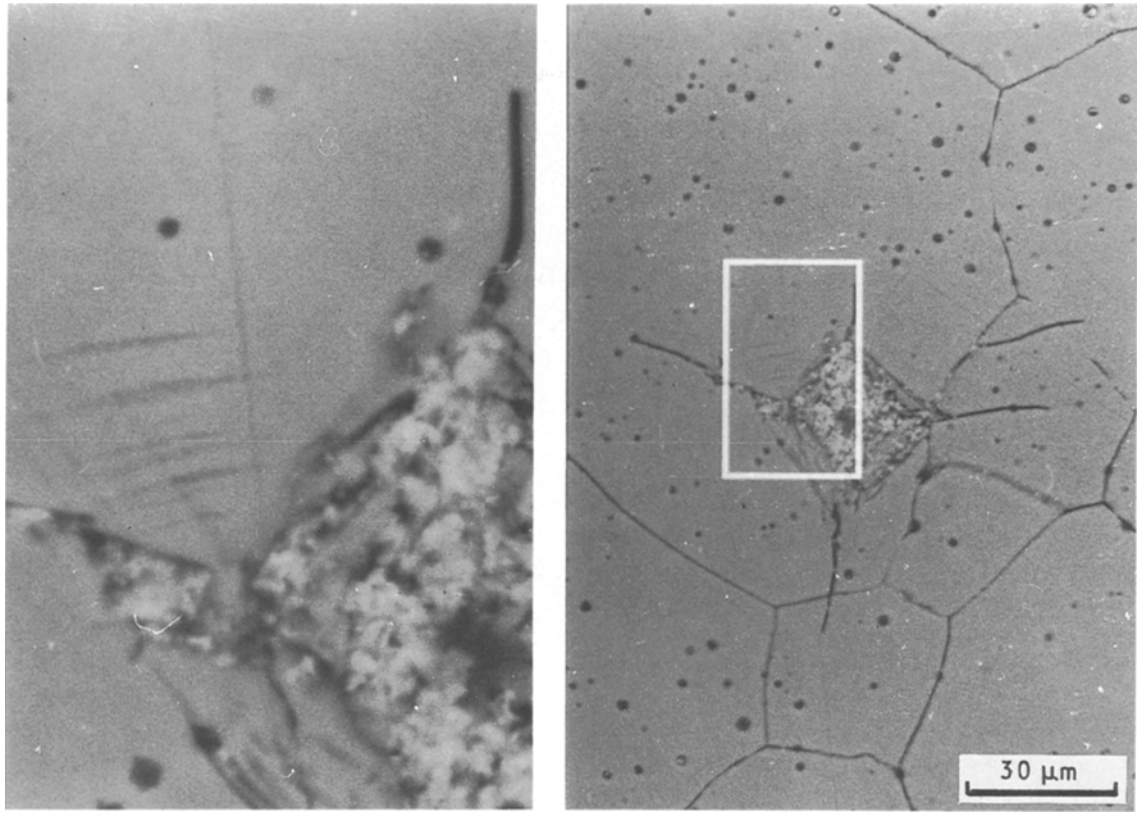

Figure 8 Back-scattered electron image of a 1 kg Vickers indentation made in CPSZ0 at room temperature. The specimen was etched in orthophosphoric acid prior to indenting.

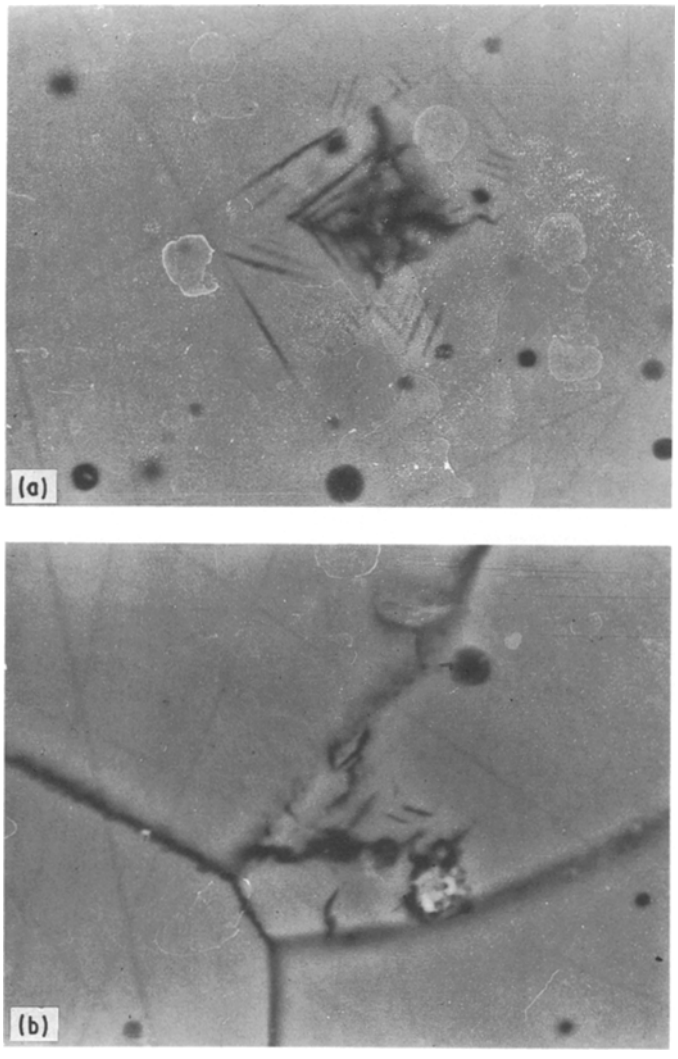

Figure 9 Secondary electron images of 10 g Vickers indentations made at room temperature in CPSZ0, (a) in the centre of a grain, (b) in the corner of a grain, (c) close to a grain boundary, (d) adjacent to a scratch.

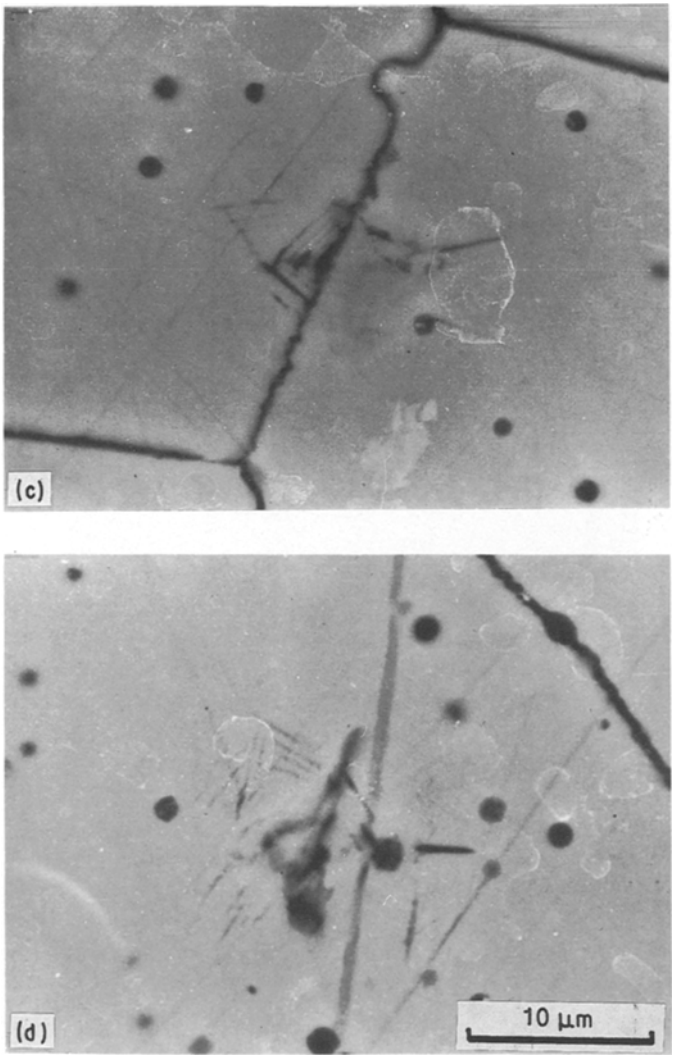

Figure 9 Continued.

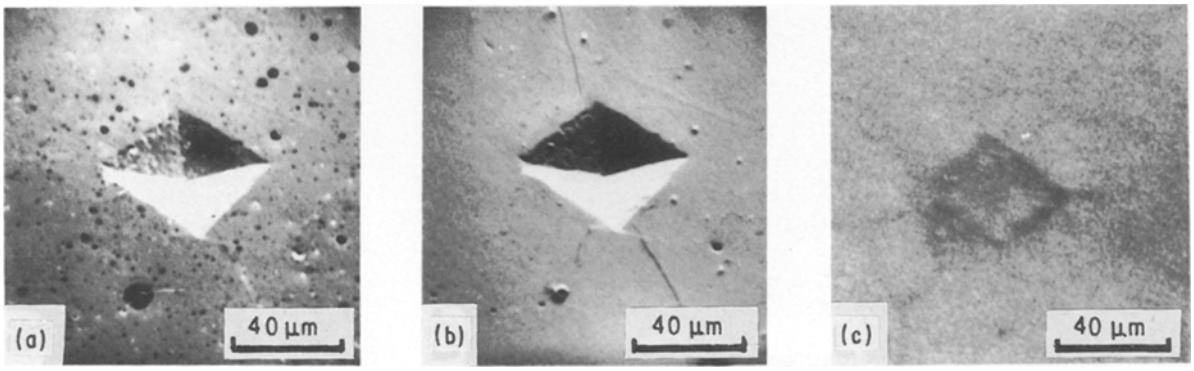

Figure 10 (a) BSE, (b) SE and (c) CL SEM images of a 1 kg Vickers indentation made at 800°C in CPSZ0.

indentor, together with a differently shaped indentor. The activation energies in Table III are lower than those for other ceramics (e.g. [14, 15]); what this signifies in terms of operating mechanisms is not clear at the moment. Because the composition of the CPSZs was identical, the temperature response of hardness must be associated with the phase distributions.

The tetragonal–monoclinic transformation is martensitic. Thus, the reduction in the size of the luminescent lobes (Figs 6 and 7) and shear bands (Figs 8 and 10) around indentations with increasing temperature is consistent with the reduction in the degree of undercooling [16]. The shear bands around indentations in CPSZ0 (Fig. 9) are seen to be influenced by microstructural features and are crystallographic in nature. That is, they do not just follow the maximum shear stress trajectories.

5. Conclusions

The hardness behaviour of four zirconia-based ceramics has been investigated as a function of contact size and temperature. As the contact size is decreased the

hardness was found to increase, generally by at least 50%. For very shallow penetrations the hardness was found to decrease rapidly. It was further observed that materials with the greatest proportion of tetragonal phase were less susceptible to this near-surface softening.

As the indentation temperature is increased the CPSZ materials all tended towards the same hardness value; extrapolation of the results suggests that they coincide at the eutectoid temperature. MPSZ has a slightly higher eutectoid temperature but also tends to a similar hardness value.

SEM examination of the deformation structures surrounding the indentations was performed. Shear bands were observed around room-temperature indentations in CPSZ0. The generation and extent of these shear bands was strongly influenced by grain boundaries. As the temperature of indentation was increased their extent decreased, such that at 800 °C none were observed. For MPSZ, lobes of transformed monoclinic were observed around room-temperature indentations. Again, as the indentation temperature was increased their extent decreased; at 800 °C the transformed zone was limited solely to the indentation site.

Acknowledgements

The authors thank Professor R. W. K. Honeycombe for the provision of laboratory facilities. M. V. Swain, CSIRO (Melbourne), kindly provided the materials. J.T.C. acknowledges an award from SERC under the CASE scheme in collaboration with I.C.I. (Fibres), Harrogate.

References

1. R. H. J. HANNINK and R. C. GARVIE, *J. Mater. Sci.* **17** (1982) 2637.
2. R. H. J. HANNINK, K. A. JOHNSTON, R. T. PASOE and R. C. GARVIE, in "Advances in Ceramics", Vol. 3, "Science and Technology of Zirconia" edited by A. H. Heuer and L. W. Hobbs (American Ceramic Society, Columbus, OH, 1981) pp. 11–36.
3. N. CLAUSSEN, *Proc. Brit. Ceram. Soc.* **34** (1984) 157.
4. P. M. SARGENT and T. F. PAGE, *ibid.* **26** (1978) 209.
5. M. G. S. NAYLOR and T. F. PAGE, *J. Microsc.* **130** (1983) 345.
6. A. G. ATKINS, A. A. DOS SILVERIO and D. TABOR, *J. Inst. Metals* **94** (1966) 369.
7. J. T. CZERNUSZKA and T. F. PAGE, *J. Amer. Ceram. Soc.* **68** (1985) C196.
8. R. H. J. HANNINK and M. V. SWAIN, *J. Mater. Sci.* **16** (1981) 1428.
9. R. STEVENS, *Magnesium Elektron Publ.* **113** (1983).
10. R. P. INGEL, D. LEWIS, B. A. BENDER and R. W. RICE, in 'Advances in Ceramics", Vol. 12, "Science of Technology of Zirconia 2", edited by N. Claussen, M. Ruhle and A. H. Heuer (American Ceramic Society, Columbus, OH, 1984) p. 408.
11. J. T. CZERNUSZKA, PhD Thesis, Cambridge University (1985).
12. J. H. WESTBROOK and P. J. JORGENSEN, *Trans. Met. Soc. AIME* **233** (1965) 425.
13. R. H. J. HANNINK and M. V. SWAIN, in "Materials Science Research", Vol. 18, "Deformation of Ceramic Materials 2", edited by R. E. Tressler and R. C. Bradt (Plenum, New York, 1984) p. 69.
14. J. T. CZERNUSZKA and T. F. PAGE, *J. Mater. Sci.* **22** (1987) 3907.
15. M. G. S. NAYLOR and T. F. PAGE, 3rd Annual Technical Report USAERO, Grant No. DA-ERO-78-G-010 (1981).
16. D. A. PORTER and K. E. EASTERLING, "Phase Transformations in Metals and Alloys" (Van Nostrand Reinhold, Wokingham, UK, 1981).

Received 22 May
and accepted 3 June 1991